CrossMark

RESEARCH ARTICLE

Dynamic implications of ridges on a debris avalanche deposit at Tutupaca volcano (southern Peru)

Patricio Valderrama[1,2] · Olivier Roche[2] · Pablo Samaniego[2] ·
Benjamin van Wyk de Vries[2] · Karine Bernard[2] · Jersy Mariño[1]

Abstract Catastrophic volcanic landslides can involve different parts of a volcano that can be incorporated into any resulting debris avalanche. The different material properties may influence the mechanical behaviour and, hence, the emplacement mechanisms of the different avalanche units. We present data from a coupled hydrothermal- and magmatic-related volcanic landslide at Tutupaca volcano (Peru). Around AD 1802, the hydrothermal system under Tutupaca's growing dacite dome failed, creating a debris avalanche that triggered a large explosive eruption. A typical debris avalanche hummocky unit is found, formed out of rock from the dome foot and the underlying hydrothermally altered lavas. It is covered by a more widespread and remarkable deposit that contains remnants of the hot dome core and the inner hydrothermal material. This deposit has ridges 20–500-m long, 10–30-m wide and 1–5-m high, regularly spaced and that fan slightly outward. Cross sections exposed within the ridges reveal coarser cores and finer troughs, suggesting grain size segregation during emplacement. Ridge morphology and granulometry are consistent with fingering known to occur in granular flows. The ridges are also associated with large blocks that have evidence of differential movement compared with the rest of the flowing mass. The presence of both ridged and hummocky deposits in the same event shows that, as different lithologies combine and collapse sequentially, materials with different mechanical properties can coexist in one landslide, leading to contrasting emplacement dynamics. The different structures thus highlight the complexity of such hazardous volcanic events and show the difficulty we face with modelling them.

Keywords Tutupaca volcano · Debris avalanche · Flank collapse · Ridges · Granular fingering

Introduction

Volcanic landslides and debris avalanches associated with magmatic and hydrothermal activity, such as Mount St. Helens (1980) or Bandai San (1888), represent major volcanic hazards (Siebert 1984; Siebert et al. 1987). Because of the complex mix of different rock types, fluids and gasses, resulting debris avalanches are likely to have complex and variable mechanical properties that control avalanche emplacement and run out distance (e.g. Voight et al. 2002; Shea and van Wyk de Vries 2008; van Wyk de Vries and Davis 2014; Roverato et al. 2015). These mechanical differences to mobility must be taken into account when assessing their impacts. The rock of the collapsing volcanic edifice can be hot and can contain water and gas while the hydrothermally altered material has abundant fines and clays as well as water. Both magmatic and hydrothermal materials may fragment easily to produce a wide range of particle sizes, which can control the emplacement mechanism of the avalanche (Eppler et al. 1987; Glicken 1998; Voight et al. 2002; Legros 2002). Particle size segregation can promote segregation features, while in fine material with low hydraulic permeability, water and gas could provide interstitial pore fluid pressure for the moving mass as shown for example for debris flows (Iverson 1997). The incorporation of variable amounts of fresh

✉ Patricio Valderrama
pvalderrama@ingemmet.gob.pe

[1] Observatorio Vulcanológico del INGEMMET (OVI), Av. Canada 1470, San Borja, Lima, Peru

[2] Laboratoire Magmas et Volcans, Université Blaise Pascal - CNRS - IRD, OPGC, TSA 60026 - CS 60026, 6 Avenue Blaise Pascal, 63178 Aubière, France

Springer

rock, hot magma and parts of the hydrothermal system is likely to cause different mechanical behaviours for different flowing sections of an avalanche.

Surface features on debris avalanche deposits have been used to determine their kinematics and to suggest their emplacement dynamics (Belousov et al. 1999; van Wyk de Vries et al. 2001; Kelfoun and Druitt 2005; Dufresne and Davies 2009; Paguican et al. 2014). These features are either hummocks and megablocks (e.g. Paguican et al. 2014), extensive fault and fold networks (e.g. Shea and van Wyk de Vries 2008), or elongated ridges (e.g. Belousov et al. 1999; Dufresne and Davies 2009). While hummocks and faults have been carefully analysed in debris avalanche deposits (Clavero et al. 2002; Paguican et al. 2014), ridges have not been examined in detail in the field in relation to structure and sedimentology, even though they are likely to provide clues to the processes involved in avalanche emplacement.

In this work, we describe the surface features observed in a young and well-preserved volcanic debris avalanche deposit of Tutupaca volcano in southern Peru. In particular, we report a quantitative analysis of ridge morphology, as well as granulometry in two selected trenches dug across the ridges. These data have been compared with those of experiments on granular flows that allow us to discuss the implications of ridge formation for debris avalanches emplacement dynamics.

The Tutupaca volcano and its recent deposits

The Tutupaca volcanic complex in southern Peru (Figs. 1 and 2) is composed of an old, highly altered and eroded and glaciated basal edifice and two younger twin peaks, located in the northern part of the complex (the western and eastern Tutupaca; Samaniego et al. 2015). The younger edifice of the complex, the eastern Tutupaca, is a dome complex that sits on top of the basal edifice and consists of at least seven dacitic domes with no discernible glacial erosion, which suggests that they have formed during the Holocene. The most striking characteristic of this recent edifice is the presence of a ~1-km-wide collapse amphitheatre open to the NE and a related hummocky and ridged debris avalanche deposit that spreads out on the adjacent highlands (Figs. 1 and 2).

The sector collapse scar at Tutupaca has an inner bowl shape, opening to a shallow outer scar and slide plane. The inner upper walls of the scar consist of unaltered dome lava, underlain by reddish altered dome lavas, both correlative with eastern Tutupaca domes, and highly altered lavas of the lower basal edifice. The scar opens onto a 25° inclined slope on which similarly inclined basal volcano strata outcrop under a partial cover of later collapse breccia. The base of the outer scar is composed of slightly altered lavas and intensely hydrothermally altered white and yellow zones.

Samaniego et al. (2015) described the recent deposits of Tutupaca (Fig. 3), which consist of (i) a debris avalanche deposit with two main units of different composition, structural characteristics and travel path, and (ii) a large pyroclastic density current deposit that covers the volcano's northwest base, which is interleaved with the debris avalanche deposit. Charcoal in this pyroclastic deposit has been dated at about 218 ± 14 aBP (P-PDC of Samaniego et al. 2015), which is consistent with historical accounts of eruptive activity during the eighteenth and nineteenth centuries. The stratigraphic relationship between the debris avalanche and the pyroclastic density current deposit, coupled with the petrological similarity between the juvenile fragments in the debris avalanche, the pyroclastic density current deposit and the pre-avalanche domes, indicates (1) that juvenile magma was involved in the sector collapse and (2) that the debris avalanche and the pyroclastic density currents are different phases of a single, albeit complex sequence of events. Samaniego et al. (2015) concluded that this eruption represents the youngest debris avalanche in the Andes and was accompanied by one of the largest explosive events to have occurred in Peru during historical times.

The debris avalanche deposit description

Unit characteristics and terminology

The debris avalanche deposit (DAD) is exposed in the NE part of Tutupaca between the amphitheatre and the Paipatja plain, reaching 6–8 km from its source and covering an area of 12–13 km² (Fig. 1). Based on stratigraphic and lithological data, Samaniego et al. (2015) described two distinct DAD units separated by the Paipatja pyroclastic density current deposits (P-PDC) (Fig. 3). The lower unit is mostly composed of hydrothermally altered lava fragments as well as minor amounts of oxidized dome lavas, and it is referred to as the hydrothermally altered debris avalanche deposit (HA-DAD, Fig. 3). The upper unit is mostly composed of unaltered (fresh) dome fragments, which grade from sand-size particles to several meters in size. This unit is characterized by abundant prismatically jointed blocks that have been interpreted to be juvenile dome fragments, and has been called the dome-rich debris avalanche deposit (DR-DAD, Fig. 3).

In this study, we define units based on surface features and structures rather than lithology because our aim is to discuss the emplacement dynamics of the debris avalanche from the characteristics of these structures (Fig. 3). Based on these morphological features, we distinguish two main DAD units. The lower unit 1 spreads between the amphitheatre and the Paipatja plain and is confined by the old glacial valleys over most of its path. At the foot of the amphitheatre, unit 1 is characterized by an inner 1–1.5-km-wide and 100–200-m-thick toreva-like structure and it grades outwards to a series of hectometric
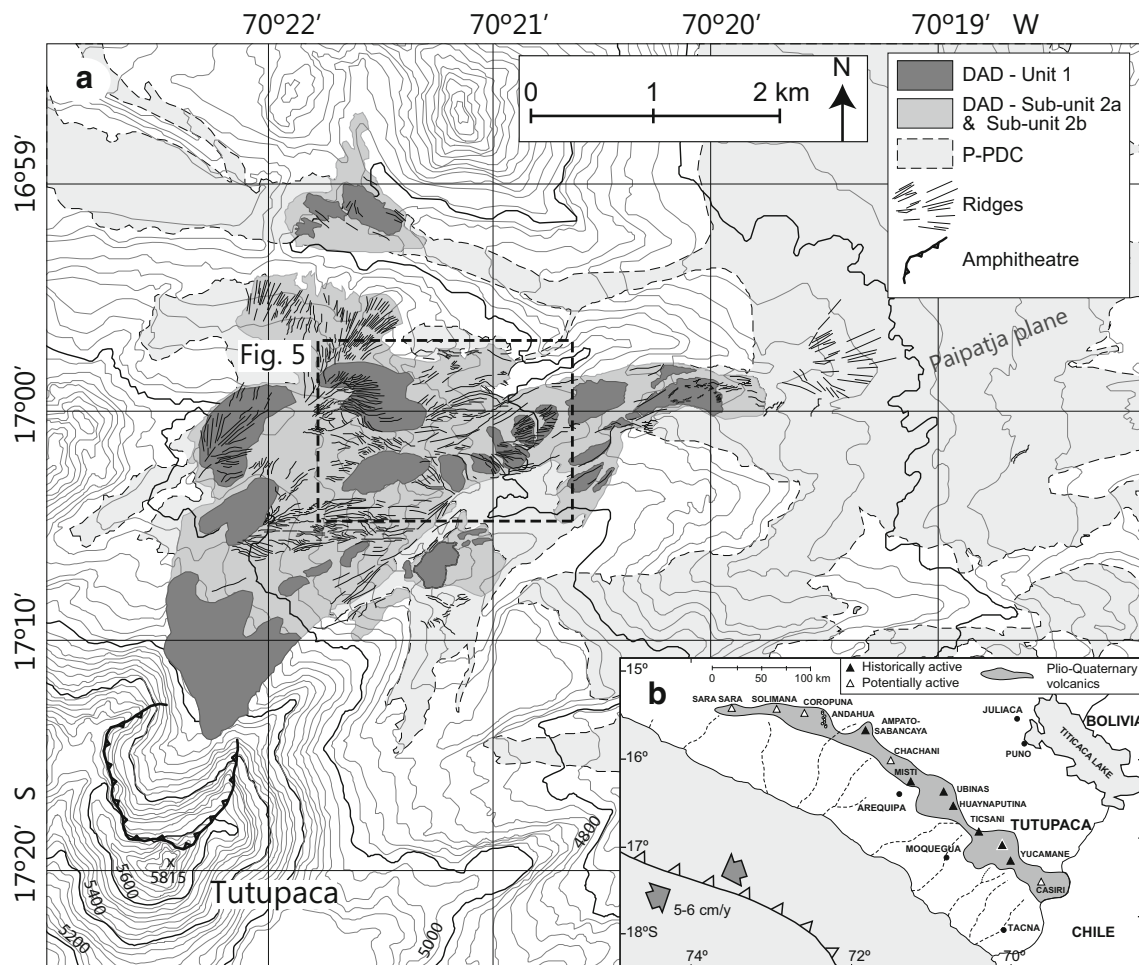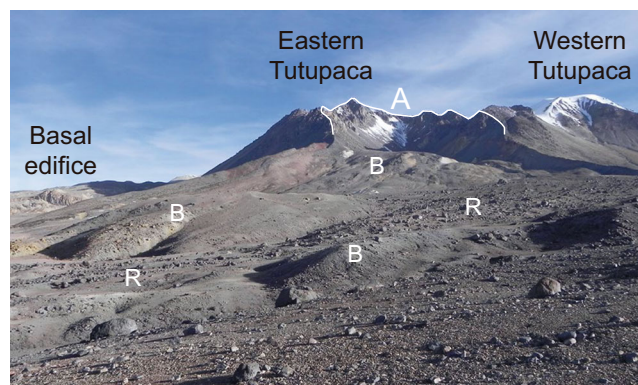
Fig. 1 **a** Map of Tutupaca debris avalanche deposit (DAD), showing the lower hummocky unit 1 and the more extended, upper ridged unit 2. *P-PDC* stands for the Paipatja pyroclastic density current deposit. Location of image presented in Fig. 5 is indicated. **b** Location of the Tutupaca volcano in the Peruvian volcanic arc

debris avalanche blocks (cf. Glicken 1991) as well as smaller hummock-like hills (Figs. 1 and 2). This hummocky debris avalanche deposit outcrops up to 4–6 km from the amphitheatre. The structures preserve the partially intact

Fig. 2 Panoramic view of the Tutupaca volcano with amphitheatre (*A*) open to the NE, debris avalanche blocks (*B*) of Unit 1 and ridges (*R*) of the unit 2

original stratigraphy (Figs. 2 and 3) with a lower hydrothermally altered layer overlain by a unit composed of older volcanic edifice and recent dome lava. This deposit has the characteristics of a classic volcanic debris avalanche (e.g. van Wyk de Vries and Davies 2014).

In contrast, the thinner overlying breccia unit 2, that outcrops up to 5–7 km from the amphitheatre, is notable for its ridged surface (Figs. 1 and 2). This unit varies in surface lithology and is divided it into two sub-units (Fig. 3). The widespread sub-unit, 2a, mostly contains white and yellow hydrothermally altered lava, with clast fragments smaller than 10 cm, and sparse large, massive megaclast up to 5–10 m in diameter. The other sub-unit, 2b, is only found in the central part of the deposit, which is mostly channelized in a glacial valley running to the east from the Tutupaca base to the Paipatja plain (Fig. 3a). This sub-unit is composed of unaltered (fresh) dark grey dome rocks of dacitic composition. Neither sub-unit 2a nor sub-unit 2b has a clearly defined internal stratigraphic sequence, as can be seen from the two
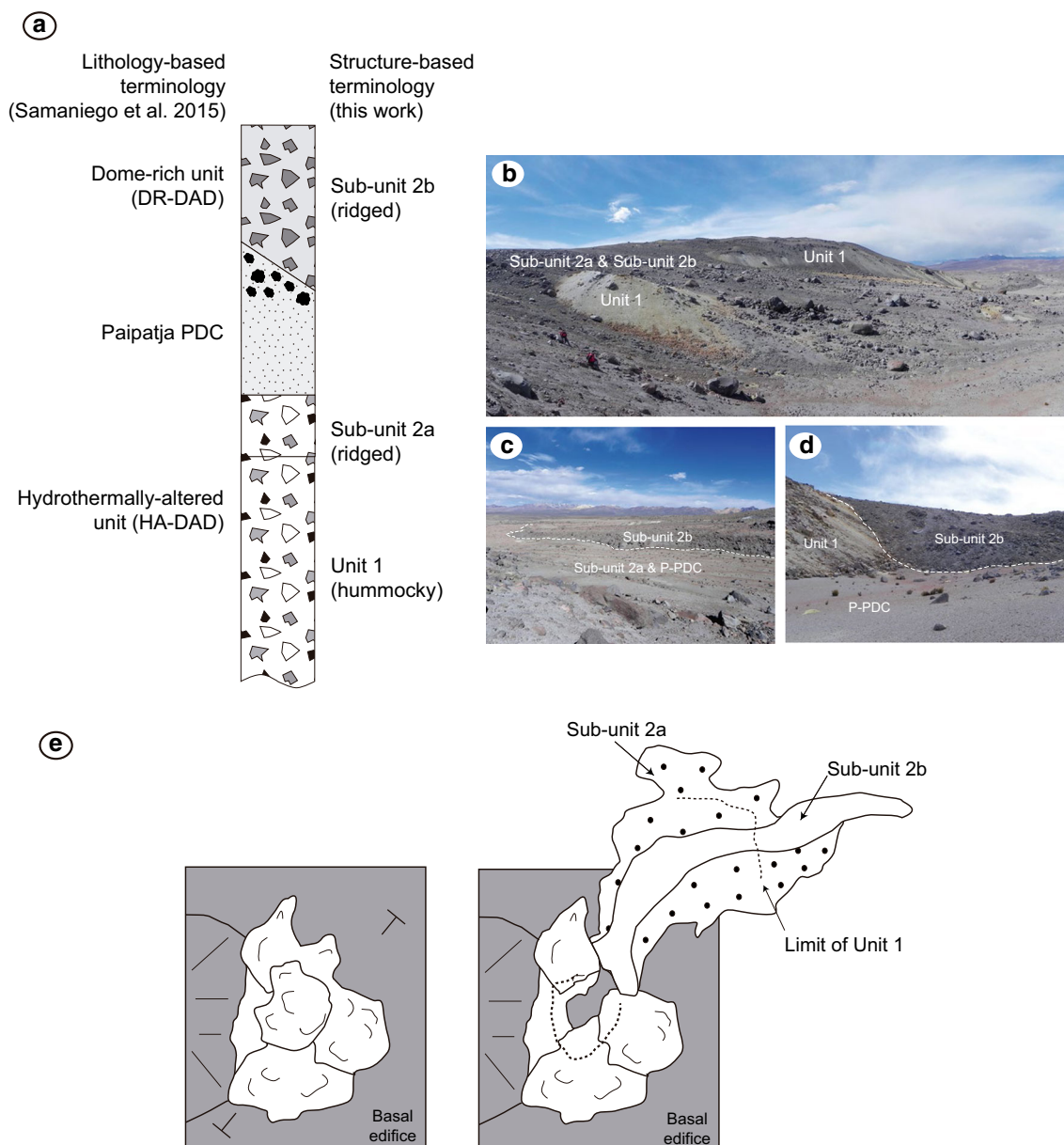
Fig. 3 **a** Composite stratigraphic section showing the units terminology used in this work and by Samaniego et al. (2015). **b** Panoramic view of both debris avalanche deposits: the lower hummocky unit 1 and the upper ridged unit 2 (sub-units 2a and 2b). **c, d** Photographs showing the contacts between the different units. **e** Simplified sketches showing the Tutupaca volcano before and after the collapse and the spatial distribution of the debris avalanche deposits

trenches we excavated and from few other exposures of the interior. It is worth noting that the contact between the underlying unit 1 and the overriding sub-units 2a and 2b can only be seen at scarce outcrops such as those shown in Fig. 3.

The lithologies present in the debris avalanche deposit units and their distribution correspond to lithologies in the scar. Unit 1 and sub-unit 2a (i.e. HA-DAD of Samaniego et al. 2015) fits with the lithologies seen in the lower part of the scar and the scar inner east side, which mostly correspond to the basal edifice or the lower part of the Tutupaca domes. In contrast, the lithologies observed in sub-unit 2b (i.e. DR-DAD of

Samaniego et al. 2015) correspond to those observed in the scar inner west side, which correspond to the young Tutupaca domes.

Deposits of the P-PDC that accompanied the collapse are found on top of the avalanche unit 1 and sub-unit 2a in most areas, whereas they are overlain by the upper dome-rich sub-unit 2b (Fig. 3). These PDC deposits are thickest in the inter-ridge depressions, where we excavated down to 1.5 m without being able to find the avalanche deposit below. The P-PDC was deposited around large blocks and accentuates the appearance of the ridges.

Surface structures

Quantitative morphological data on the surface structures were measured from georeferenced Google Earth® Pro images with a pixel resolution of 5 m. The surface morphology of unit 1 is characterized by 200–700-m-long and 20–40-m-high debris avalanche blocks as well as smaller 100–200-m-long hummock-like hills (Fig. 2). These features outcrop in the medial zone, between ~2 and ~6 km from the amphitheatre. In contrast, unit 2 is composed of abundant ridges that are elongated, subparallel elevations separated by depressions on the surface of the avalanche deposit (Figs. 2, 3 and 4). These ridges are most abundant between 4 and 5 km from the scar, but are also present in the distal regions where they are partially buried by the P-PDC deposit (Fig. 1). In this study, 30–35 % of ridges are composed of the sub-unit 2a and the remaining 65–70 % occur within the dome-rich sub-unit 2b. The morphological characteristics of the ridges are presented in Fig. 5. The length of the ridges varies from a few meters to more than 500 m, with an average of 100 to 150 m

(Fig. 5c). There is no relationship between the length of the ridges and their distance from the scarp (Fig. 5f). The ridges are 10–30-m wide, and the separation of the ridge axis (or wavelength) varies from ~30 to 35 m in the proximal area but reaches up to ~60 m at 6 km from the scar in open areas where the deposit has fanned out. The ridge height was measured in the field. They are typically 1–5-m high, and the largest ridges (>3-m high) are within the fresh sub-unit 2b near the proximal region. No relationship between the size and the ridge lithology is found.

A notable feature of the ridges in unit 2 is the concentration of larger blocks on the ridge crests (Figs. 3, 4 and 6). The ridge surfaces in the altered sub-unit 2a are smooth, either simple one-summit ridges with 10 to 20° side slopes, or multiple ridges, or flattopped ridges between two deep troughs. The height of the ridges increases progressively along strike after initiation and also tend to decrease gradually. Some ridges start abruptly downstream from large blocks (3–30-m wide), giving a tail-like aspect, while others have blocks up to 10 m in diameter along the axis of the ridge (Fig. 6).

Fig. 4 Photograph showing the different surface morphologies of the DAD units 1, 2a and 2b. Note people and cars for scale. **a** Elongated ridges on sub-unit 2a. **b** Ridges on sub-unit 2b. Note the important amount of block on these ridges, compared with those of the sub-unit 2a. **c** Hummock field on unit 1 covered by ridged sub-unit 2a. **d** Trench dug in a ridge of the medial part of the DAD sub-unit 2a. **e** Blocks on top of the ridged sub-unit 2a
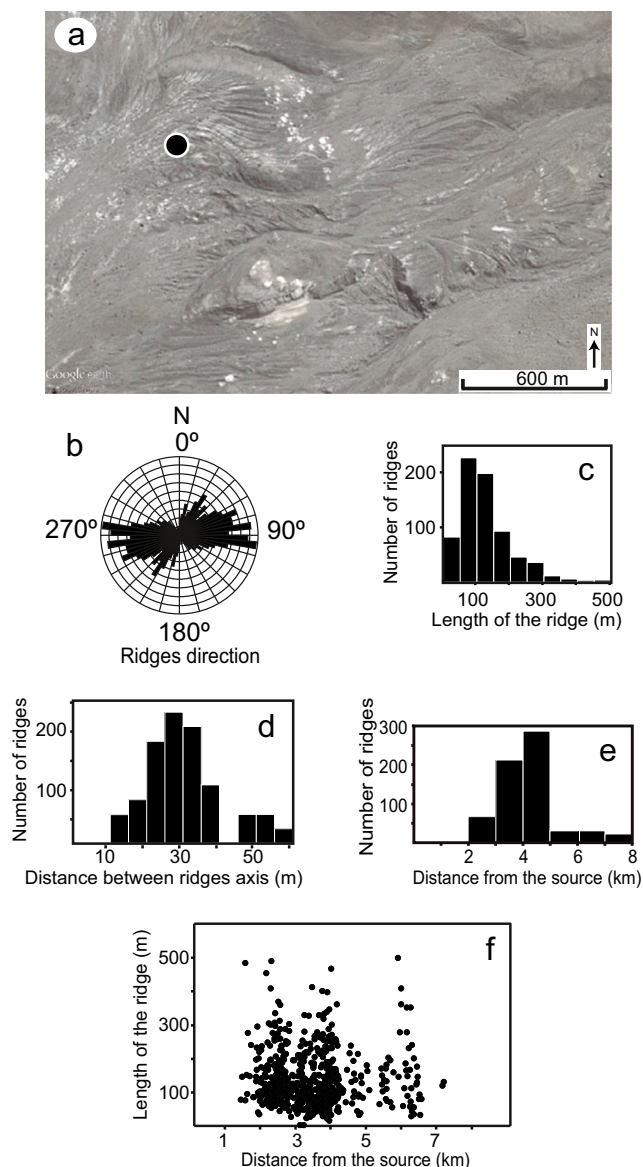
Fig. 5 **a** Google Earth® image of the ridges (location given in Fig. 1). The *black dot* corresponds to the location of the trenches dug across the ridges and presented in Fig. 7. **b** Rose diagram showing the ridge directions. **c–e** Histograms showing the morphological characteristics of ridges. **f** Diagram showing the length of the ridges as a function of the distance from the source

Concentrations of smaller blocks are found either downstream or upstream of the largest blocks. It was observed that these smaller blocks are pushed together, with trapped, brecciated blocks in between larger ones (Fig. 6). Impact marks were frequently seen. Some large blocks had zones of bulldozed matrix in front or behind the block, on all parts of the deposit.

Sedimentological data of elongated ridges

Two trenches were excavated to expose the interior of two ridges in the sub-unit 2a (Fig. 7). The internal upper 2 m of

both ridges showed a similar structure, with a central zone of slightly coarser breccia and steep-sided contacts with an inter-ridge filling of later pyroclastic flow material. In both trenches, there was an altered upper layer at the centre that thinned at the ridge edge, and there were some indistinct lenses of different coloured breccia and some wedges or breccia-filled cracks. Facies exposed in the trenches were sampled and analysed for granulometry, component and textural analysis. Forty-nine, noncohesive samples were sieved to establish the grain-size distribution using the method of Blott and Pye (2001) and their Gradistat software. From this analysis, the matrix of the sampled material was defined at <32 mm.

The ridge structure and the material characteristics are shown in Fig 7. The contacts between the fresh and altered material in the central part of the ridge are lobate and steeply inclined outwards on the left side (facing uphill) where a red facies in the fresh breccia is also in contact with a brown material (Fig. 7a, b). On the right side (facing uphill) the contacts are convolute, with a fluidal-like mixing of brown fresh and yellow altered materials. The pyroclastic density current material is also involved in this mixing, down to a few centimetres below the contact (Fig. 7a, b). Histograms of the size distribution of the breccia matrix show that the samples are sand to gravel size dominated and fines poor (Fig. 7c). The pyroclastic density current deposit grain size distribution is notably different, with less sorting and more fines. The cumulative curves (Fig. 8) further show, with a few exceptions, a continuous change in size range from between the more poorly sorted and finer samples outside the ridge axis to the better sorted and coarser central breccias at the ridge axis. Angular andesitic breccia clasts with planar faces and subrounded cauliflower-like dense clasts are found to be predominant in the ridge axis (Fig. 7d). The breccia clasts are more rounded in the lateral parts of the ridge, where some clasts are coated in fine hydrothermal clays and deeply oxidized, giving a more rounded shape.

Discussion

The distribution of the lithologies within the deposits suggest that the debris avalanche at Tutupaca initiated with a failure of the lower hydrothermal system that allowed a frontal and basal avalanche unit (unit 1) to form (Fig. 9). Behind this, parts of the growing lava dome, with its hot magma carapace and part of the inner hydrothermal system, failed to produce units 2a and 2b. Such a sequence is similar to that seen in the Rosenquist slides of Mount St. Helens (Lipman and Mullineaux 1981) and reproduced in analogue models of Andrade and van Wyk de Vries (2010) and Paguican et al. (2014). We now discuss dynamical implications of the structures observed, focusing on the ridged deposits, that present a

Fig. 6 Relationships between ridges and large (typically >10 m) blocks. The direction of movement is from the *left* to the *right*. **a** Map view and cross section of configurations I, II, and III between large and small blocks. Small blocks are concentrated downstream or upstream of the large blocks. **b** Photograph and interpretation of configuration II
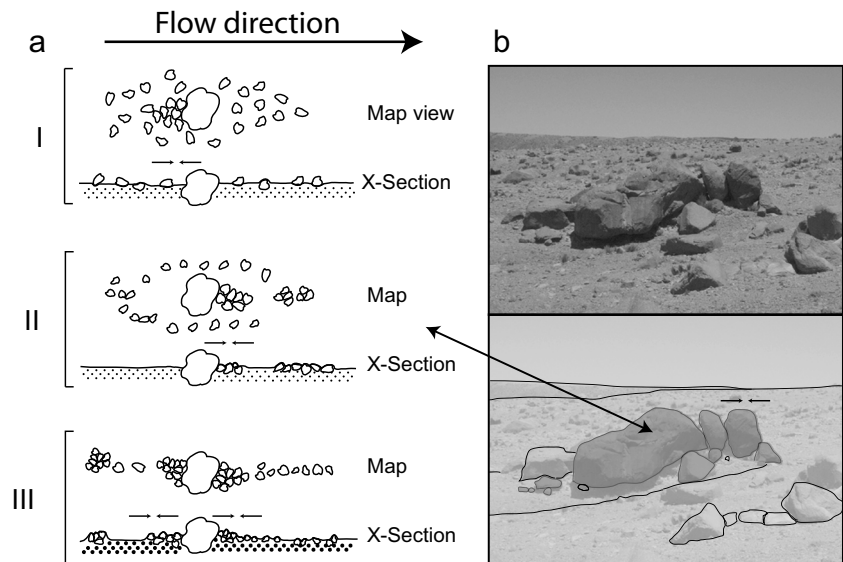
significantly different type of surface structure to that seen on most hummocky volcanic debris avalanche deposits.

## Comparison with other ridged debris avalanche deposits

Elongated ridges (or flowbands following the terminology of Dufresne and Davies 2009) have been described at the debris avalanche deposits of Shiveluch (Belousov et al. 1999) as well as some other volcanic debris avalanche deposits in the Central Andes such as those of Socompa (Kelfoun et al. 2008; van Wyk de Vries et al. 2001), Llullaillaco (Richards and Villeneuve 2001) and Lastarria (Naranjo and Francis 1987). Similar features have been also described in non-volcanic environments, such as landslides (Shaller 1991) and rock avalanches overriding glaciers (McSaveney 1978), as well as in extraterrestrial environments (i.e. Mars, Luchitta 1978; Shaller 1991). The 1964 Shiveluch deposits in particular show strong similarities with those of the Tutupaca debris avalanche. Like Tutupaca, the medial and distal part of the Shiveluch debris avalanche deposit display abundant elongated, subparallel ridges and depressions, whose dimensions (i.e. 1–30-m wide, 0.3–10-m high and up to 1-km long, Belousov et al. 1999) are of the same order of magnitude than at Tutupaca. Belousov et al. (1999) interpret these ridges and depressions as a result of unconfined spreading of a laminar plug flow that produces radial extension of the avalanche. However, Belousov et al. (1999) does not provide a detailed field description of the lithologies or internal structure of the ridges.

Interpretation of Tutupaca ridges

Ridge-like structures showing particle grain size segregation have been observed to form in experiments on polydisperse granular flows exhibiting granular fingering (Pouliquen et al.

1997; Pouliquen and Vallance 1999; Mallogi et al. 2006; Gray and Kokelaar 2010; Johnson et al. 2012). Flow fingers form when larger, more angular particles first segregate at the flow surface, as a response to size-induced percolation of fines and squeeze expulsion (Fig. 10). These larger particles then travel faster than the rest of the flowing mass and concentrate at the flow front. Small perturbations cause deflection of the trajectories of these large particles along the steepest surface slope, which causes formation of frontal lobes and emerging static lateral levées. Localized concentrations of these large particles result in a larger friction coefficient leading to local flow deceleration, which favours amplification of the instabilities and leads to the emplacement of granular fingers with lateral levées enriched in coarse material. Recirculation motion of the coarse particles (see also Johnson et al. 2012) can sustain the segregation process and favour the formation of long granular fingers. A notable result is that the fingers (i) are enriched in large particles at their joint margins that eventually form streamwise elongated ridges in the granular mass and (ii) have a nearly constant width, which defines a typical wavelength (i.e. length between consecutive parallel ridges).

We interpret the Tutupaca ridges as joint margins of the lateral levées of granular fingers where the large blocks were concentrated. In this context, inter-ridge depressions formed as the flowing granular mass drained the central part of the fingers that became progressively less elevated than the ridges, as shown for self-channelling granular flows depicting levée-channel morphology (Félix and Thomas 2004; Lube et al. 2007; Mangeney et al. 2007; Jessop et al. 2012). These depressions served as preferential pathways for the pyroclastic flows whose deposits accumulated there and thinned towards the ridge core. The segregation process observed in experiments can explain most of the observed Tutupaca ridges, particularly those whose axis separation reveals a well-defined wavelength. Furthermore, the sedimentological data show that
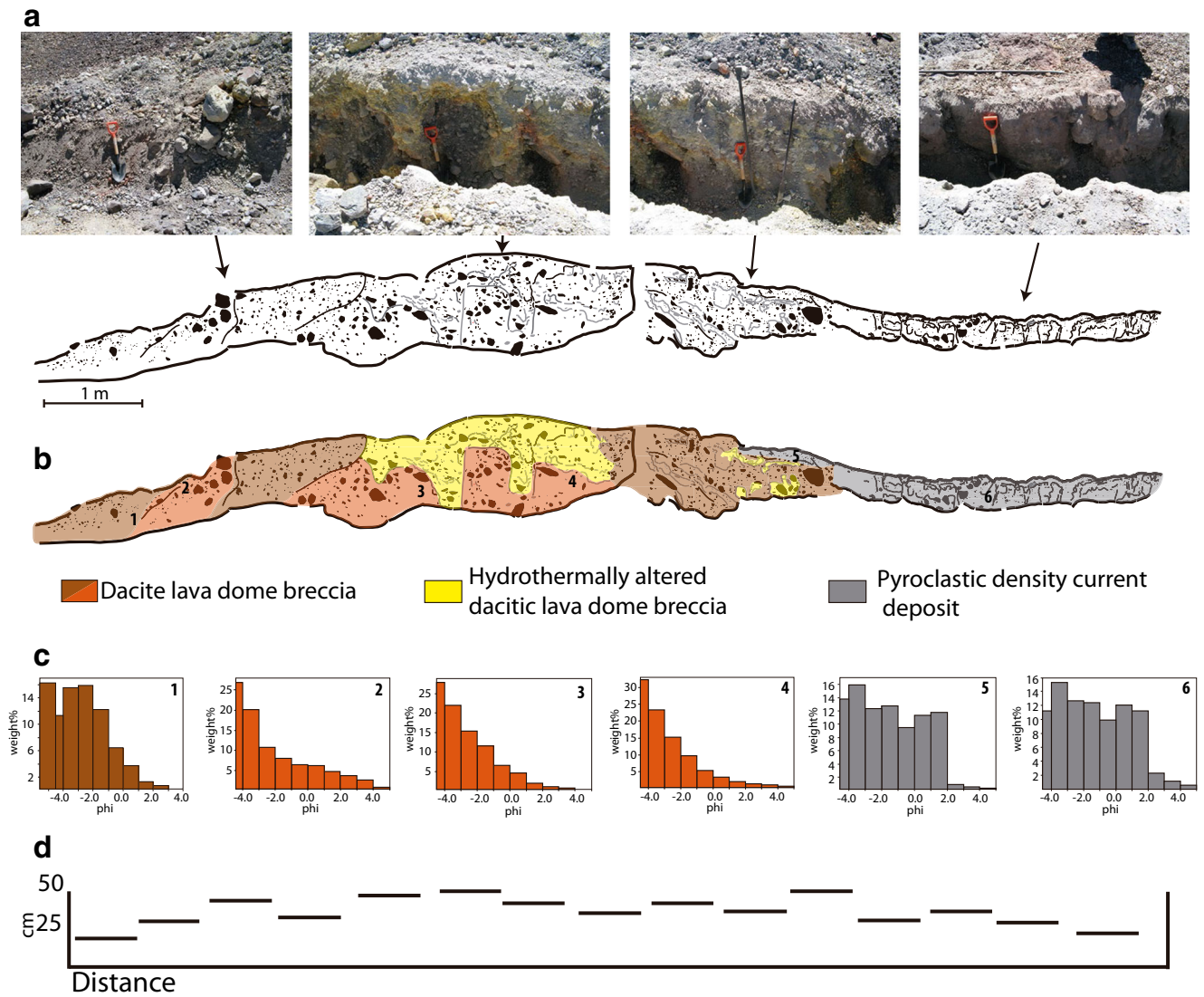
Fig. 7 **a** Sketch depicting the 1–1.5-m-high, 8–10 m-long cross section of a ridge of the unit 2a. A photo of the ridge and its location are shown in Figs. 4d and 5a, respectively. The sketch represents the ridge (facing uphill). *Irregular black dots* symbolize blocks, and *thin grey lines* represent contacts and/or structures. Photographs show the different parts of the ridge. **b** Interpretation of the different sections of the ridge according to distinct facies. Note the contact between the DAD breccia and the PDC deposit. **c** Histograms of matrix granulometry of parts 1–6 of the ridge as shown in b. **d** Maximum block size across the ridge showing the difference between the coarser core and the finer lateral parts of the ridge

Fig. 8 Cumulative grain size curves for the matrix samples collected in both trenches. Note the enrichment in coarse material in the middle (core) zone compared with the lateral zones
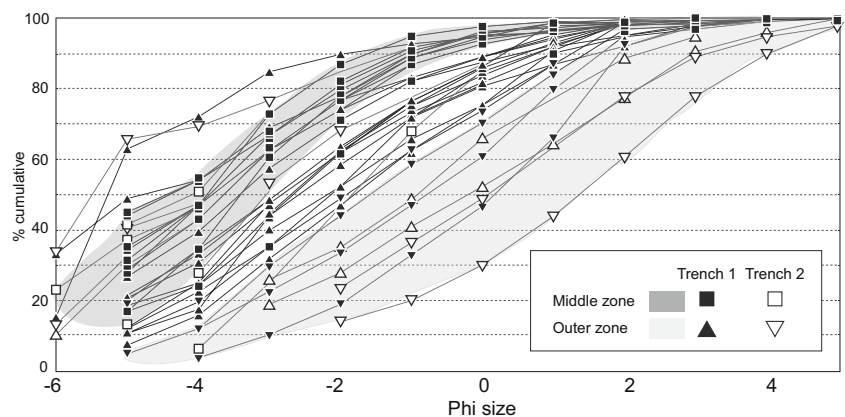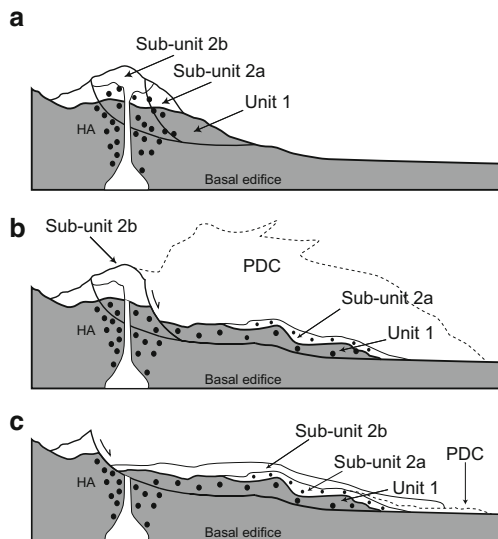
Fig. 9 a–c Sequential evolution of the Tutupaca sector collapse. Correspondence between debris avalanche units and the rock sequences at the edifice are indicated

there is a gradual change of grain size distributions, with the ridge core coarser and better sorted that the margins (Figs. 7 and 8). Textural evidence suggests that cataclasis could have also contributed to change the grain size distribution along motion. Better sorting in the ridge core may indicate that this part was the most stable (possibly static), and that granular size segregation could be preserved there, whereas the least sorted marginal zones with mixing textures, sharp fault-like boundaries and differential lateral movements suggest a

higher degree of cataclasis with much larger shear strain than in the ridge core. These features are consistent with static levées bordering a channel in which the granular material flowed. Once formed, the ridges could evolve by continued differential shear along structures as seen frequently in debris avalanches (Shea and van Wyk de Vries 2008; van Wyk de Vries and Davis 2014; Roverato et al. 2015), and by spreading of the granular mass, which accounts for the increase of separation of the ridge axes with distance.

Many ridges are associated with, or start at, greater than a meter-sized blocks (Figs. 4 and 6), as shown by differential movement of the blocks with respect to the body of the avalanche. This suggests that this differential movement may have contributed also to the initiation or development of some ridges. A block moving faster or slower than the main mass would generate a local forward or backward force. This force could then generate the constriction by impacted and accumulated block lines. The steep contacts seen in the trenches may be strike-slip faults that accommodate differential constriction in the transport direction. The role of both granular fingering and differential block movements are compatible, and could have contributed contemporaneously to ridge formation and evolution.

Dynamic implications of contrasting landslide surface textures

The Tutupaca debris avalanche deposit has two distinct structural units. The first is a 'classic' debris avalanche with
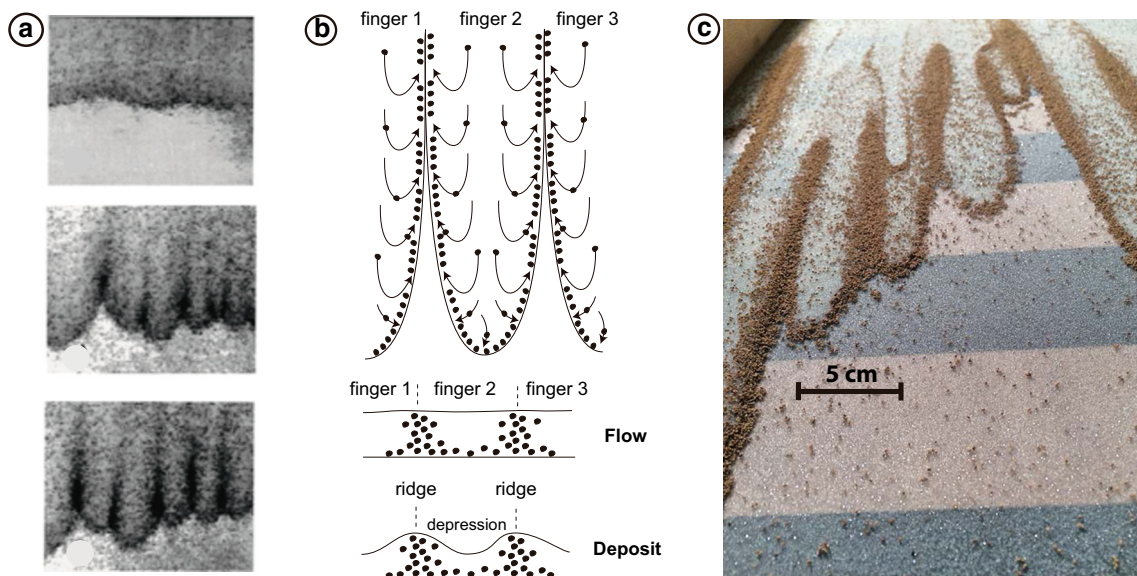
Fig. 10 a Temporal evolution of a granular flow in experiments (modified from Pouliquen and Vallance 1999). The camera is moving at the same speed as that of the flow front. Note the formation of digitation (fingers) whose lateral sides (levees) enriched in coarse material merge to form ridges. **b** Schematic representation of the ridges. The merging of lateral levees of two different fingers (top) generates ridges between depressions that form once the material is drained (see *bottom*, cross sections in flow and deposit). **c** Photograph of an unpublished experiment showing granular fingering. Larger, segregated brown particles (560–710 μm) form ridges bordering depressions white particles (300–400 μm)

hummocks, showing all the features associated with a translational slide type of emplacement. The second, ridged facies, in contrast, shows evidence of behaviour as a granular flow. The reason for this different mechanical behaviour is probably found in the different source rock, according to the collapse scenario we consider. From the scar shape, its outcrops, and from the distribution of lithology in the avalanche deposit, we propose that the landslide started as a failure in the outer altered basal edifice, which formed the main core avalanche (unit 1) (see Fig. 9). This first slide unit was overrun by a slice from the destabilized dome core and its altered base (unit 2). The ridged deposit sub-unit 2a is composed of this rock from the active dome and the hydrothermal system. This material collapsed and efficiently fragmented while propagating downslope, leading to a granular mass flow that fed the ridged unit. It is possible that the front and lateral parts of the sliding Unit 1 also collapsed and disaggregated during motion to create parts of the frontal more granular flow-ridged deposit. Thus, the mechanical behaviour of the units could have changed during transport.

Ridges at Tutupaca probably formed by a combination of granular fingering and differential movement in the moving mass, and evolved with grain size segregation and granular mass spreading. They evidence a flow behaviour that is not usually associated with debris avalanches (Belousov et al. 1999; Dufresne and Davies 2009) that are generally seen to be emplaced by sliding of a plug on a low friction base (Shea and van Wyk de Vries 2008; Kelfoun et al. 2008). In fact, the Tutupaca debris avalanche deposits show that there can be a dual mechanical behaviour in that both sliding of the relatively undisturbed edifice components and flowing of a little expanded granular mass can coexist in one event. We note that there are ridges on the Socompa debris avalanche (Kelfoun et al. 2008; van Wyk de Vries et al. 2001), and the duality of proximal hummock-dominated Toreva sliding to a more fluid-like granular flow behaviour in distal areas could also have occurred there. Our interpretation on avalanche dynamics should be equally applicable to ridges observed in landslide deposits in extraterrestrial environments (e.g. Luchitta 1978).

Conclusions

The historical (218 ± 14 aBP) debris avalanche deposit of Tutupaca volcano has two distinct units: a hummocky slide deposit and a ridged granular flow deposit. The two different units mostly originate from the different lithologies and varying magmatic and hydrothermal conditions in the initial edifice. The lower slide (unit 1) came from the lower volcano flank, where failure began in altered hydrothermal layers. The granular flow (units 2a and 2b) developed from the back of the landslide incorporating more of the brittle active dome core as well as active hydrothermal material. Unit 1 slid as a translational debris avalanche to maintain original gross stratigraphy

and produce a faulted body with hummocks. In contrast, unit 2 was more fragmented and travelled as a granular flow over and between the translational unit 1. The ridged surface of unit 2 may have resulted from a combination of granular flow processes: granular fingering, differential block velocities and spreading.

The bi-modal mechanical behaviour described here in a volcanic debris avalanche has important implications for modelling the hazards of such phenomena. Any predictive modelling should take into account the possibility of mass movements with various mechanical behaviours, and include different material properties in the edifice and take into account the initial landslide structure, all of which influence the complexity of the resulting volcanic debris avalanche deposit.

References

Andrade D, van Wyk de Vries B (2010) Structural analysis of the early stages of catastrophic stratovolcano flank-collapse using analogue models. Bull Volcanol 72:771–789

Belousov A, Belousova M, Voight B (1999) Multiple edifice failures, debris avalanches and associated eruptions in the Holocene history of Shiveluch volcano, Kamchatka, Russia. Bull Volcanol 61:324–342

Blott SJ, Pye K (2001) GRADISTAT: a grain size distribution and statistics package for the analysis of unconsolidated sediments. Earth Surf Process Landf 26:1237–1248

Clavero JE, Sparks RSJ, Huppert HE (2002) Geological constraints on the emplacement mechanism of the Parinacota avalanche, northern Chile. Bull Volcanol 64:40–54. doi:10.1007/s00445-001-0183-0

Dufresne A, Davies TR (2009) Longitudinal ridges in mass movement deposits. Geomorphology 105:171–181

Eppler DB, Fink J, Fletcher R (1987) Rheologic properties and kinematics of emplacement of the Chaos Jumbles rockfall avalanche,Lassen Volcanic National Park, California. J Geophys Res 92:3623–3633

Félix G, Thomas N (2004) Relation between dry granular flow regimes and morphology of deposits: formation of levées in pyroclastic deposits. Earth Planet Sci Lett 221:197–213

Glicken H (1991) Sedimentary architecture of large volcanic-debris avalanches. In: Smith GA, Fisher RV (eds) Sedimentation in volcanic settings 45: 99–106

Glicken H (1998) Rockslide-debris avalanche of May 18, 1980, Mount St. Helens Volcano, Washington. Bull Geol Soc Jpn 49:55–106

Gray JMNT, Kokelaar BP (2010) Large particle segregation, transport and accumulation in granular free-surface flows. J Fluid Mech 652:105–137

Iverson RM (1997) The physics of debris flows. Rev Geophys 35:245–296

Jessop DE, Kelfoun K, Labazuy P, Mangeney A, Roche O, Tilliere J-L, Trouillete M, Thibault G (2012) LiDAR derived morphology of the 1993 Lascar pyroclastic flow deposits, and implication for flow dynamics and rheology. J Volcanol Geotherm Res 245–246:81–97. doi:10.1016/j.jvolgeores.2012.06.030

Johnson CG, Kokelaar BP, Iverson RM, Logan M, LaHusen RG, Gray JMNT (2012) Grain-size segregation and levee formation in geophysical mass flows. J Geophys Res 117:F01032. doi:10.1029/2011JF002185

Kelfoun K, Druitt TH (2005) Numerical modeling of the emplacement of Socompa rock avalanche, Chile. J Geophys Res 110, B12202. doi:10.1029/2005JB003758

Kelfoun K, Druitt TH, van Wyk de Vries B, Guilbaud MN (2008) Topographic reflection of the Socompa debris avalanche, Chile. Bull Volcanol 70:1169–1187. doi:10.1007/s00445-008-0201-6

Legros F (2002) The mobility of long-runout landslides. Eng Geol 63: 301–331

Lipman PW, Mullineaux DR (Eds) (1981) The 1980 eruptions of Mount St. Helens, Washington (No. 1250). US Dept. of the Interior, US Geological Survey

Lube G, Cronin SJ, Platz T, Freundt A, Procter JN, Henderson C, Sheridan MF (2007) Flow and deposition of pyroclastic granular flows: a type example from the 1975 Ngauruhoe eruption, New Zealand. J Volcanol Geotherm Res 161:165–186

Luchitta BKA (1978) Large landslide on mars: geological society of America bulletin 89:1601–1609

Mallogi F, Lanuza J, Andreotti B, Clement E (2006) Erosion waves: transverse instabilities and fingering. Europhys Lett 75:825

Mangeney A, Bouchut F, Thomas N, Vilotte JP, Bristeau MO (2007) Numerical modeling of self-channelling granular flows and of their levée channel deposits. J Geophys Res Solid Earth 112, F02017

McSaveney MJ (1978) Sherman Glacier rock avalanche, Alaska, U.S.A. Rockslides and Avalanches. Elsevier, Amsterdam, pp 197–258

Naranjo JA, Francis P (1987) High velocity debris avalanche at Lastarria Volcano in the North Chilean Andes. Bull Volcanol 49:509–514

Paguican EMR, van Wyk de Vries B, Lagmay AMF (2014) Hummocks: how they from in and how they evolve in rockslide-debris avalanches. Landslides 11:67–80

Pouliquen O, Vallance JW (1999) Segregation induced instabilities of granular fronts. Chaos 9:621–630

Pouliquen O, Delour J, Savage SB (1997) Fingering in granular flows. Nature 386:816–817

Richards JP, Villeneuve M (2001) The Llullaillaco volcano, northwest Argentina: construction by Pleistocene volcanism and destruction by sector collapse. J Volcanol Geotherm Res 105:77–105

Roverato M, Cronin S, Procter J, Capra L (2015) Textural features as indicators of debris avalanche transport and emplacement, Taranaki volcano. Geol Soc Am Bull 127:3–18

Samaniego P, Valderrama P, Mariño J, de Wyk de Vries B, Roche O, Manrique N, Chedeville C, Fidel L, Malnati J (2015) The historical (218 ± 14 aAP) explosive eruption of Tutupaca volcano (Southern Peru). Bull Volcanol 77:51. doi:10.1007/s00445-015-0937-8

Shaller PJ (1991) Analysis of a large moist landslide, Lost River range, Idaho, USA. Can Geotech J 28:584–600

Shea T, van Wyk de Vries B (2008) Structural analysis and analogue modelling of the kinematics and dynamics of large-scale rock avalanches. Geosphere 4:657–686

Siebert L (1984) Large volcanic debris avalanches: characteristics of source areas, deposits, and associated eruptions. J Volcanol Geotherm Res 22:163–197

Siebert L, Glicken H, Ui T (1987) Volcanic hazards from Bezymianny- and Bandaï-type eruptions. Bull Volcanol 49:435–459

van Wyk de Vries B, Davies T (2014) Landslides, debris avalanches and volcanic gravitational deformation. In: Sigurdsson H, Houghton B, McNutt S, Rymer H, Stix J (eds) Encyclopedia of volcanoes, 2nd edition. Elsevier

van Wyk de Vries B, Self S, Francis PW, Keszthelyi L (2001) A gravitational spreading origin for the Socompa debris avalanche. J Volcanol Geotherm Res 105:225–247

Voight B, Komorowski J-C, Norton GR, Belousov AB, Belousova M, Boudon G, Francis PW, Franz W, Heinrich P, Sparks RSJ, Young SR (2002) The 26 December (Boxing Day) 1997 sector collapse and debris avalanche at Soufriere Hills Volcano, Montserrat, W.I. In: Druitt TH, Kokelaar BP (eds) The eruption of Soufriere Hills Volcano, Montserrat, from 1995 to 1999. Mem Geol Soc London 21: 363–407